

1 ***Title:***

2 Long-read isoform sequencing reveals tissue-specific isoform expression between active and
3 hibernating brown bears (*Ursus arctos*)

4

5 ***Authors:***

6 Elizabeth Tseng¹, Jason G. Underwood¹, Brandon D. Evans Hutzenbiler^{2,3}, Shawn Trojahn⁴,
7 Brewster Kingham⁵, Olga Shevchenko⁵, Erin Bernberg⁵, Michelle Vierra¹, Charles T. Robbins^{3,4},
8 Heiko T. Jansen², Joanna L. Kelley^{4,*}

9

10 ***Author Affiliations:***

11 ¹Pacific Biosciences, Menlo Park, CA, USA

12 ²Department of Integrative Physiology and Neuroscience, Washington State University, Pullman,
13 WA

14 ³School of the Environment, Washington State University, Pullman, WA

15 ⁴School of Biological Sciences, Washington State University, Pullman, WA

16 ⁵University of Delaware, Delaware Biotechnology Institute, Sequencing & Genotyping Center,
17 Suite 246, 15 Innovation Way, Newark, DE 19711

18

19 ****Corresponding Author:***

20 Joanna L. Kelley, joanna.l.kelley@wsu.edu

21

22 **Summary**

23 Understanding hibernation in brown bears (*Ursus arctos*) can provide insight into many human
24 diseases. During hibernation, brown bears experience states of insulin resistance, physical
25 inactivity, extreme bradycardia, obesity, and the absence of urine production. These states
26 closely mimic human diseases such as type 2 diabetes, muscle atrophy, renal and heart failure,
27 cachexia, and obesity. The reversibility of these states from hibernation to active season allows
28 for the identification of novel mediators with possible therapeutic value for humans. Recent
29 studies have identified genes and pathways that are differentially expressed between active and
30 hibernation seasons. However, little is known about the role of differential expression of gene
31 isoforms on hibernation physiology. To identify both distinct and novel mRNA isoforms, we
32 performed full-length RNA-sequencing (Iso-Seq) on three tissue types from three individuals
33 sampled during both active and hibernation seasons. We combined the long-read data with the
34 reference annotation for an improved transcriptome and mapped RNA-seq data from six
35 individuals to the improved transcriptome to quantify differential isoform usage between tissues
36 and seasons. We identified differentially expressed isoforms in all study tissues and showed that
37 adipose has a high level of differential isoform usage with isoform switching, regardless of
38 whether the genes were differentially expressed. Our analyses provide a comprehensive
39 evaluation of isoform usage between active and hibernation states, revealing that differential
40 isoform usage, even in the absence of differential gene expression, is an important mechanism
41 for modulating genes during hibernation. These findings demonstrate the value of isoform
42 expression studies and will serve as the basis for deeper exploration into hibernation biology.

43

44

45 **Keywords**

46 Hibernation, Brown bear, Transcriptomics, Iso-Seq, Alternative Splicing, Differential Isoform

47 Expression, Full-length transcript sequencing

48

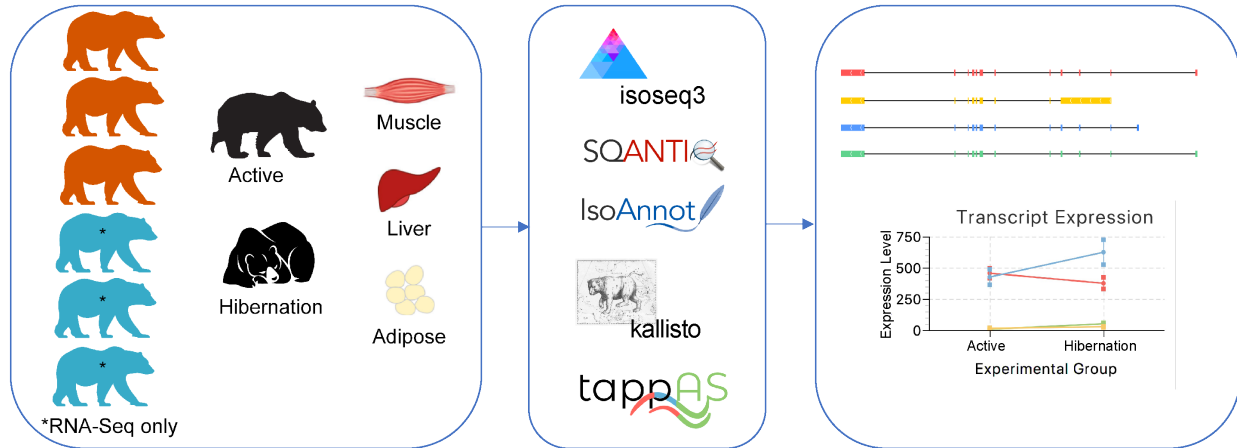
49 **Background**

50 Hibernation in bears has long been championed as a promising system for understanding the
51 extremes of mammalian physiology and for identifying novel therapeutic targets [1, 2]. Annual
52 hibernation in brown bears (*Ursus arctos*) involves massive physiological shifts to conserve
53 energy during the food-scarce winter [3], and every organ system in bears demonstrates a suite of
54 adaptations driven by the needs of hibernation. Hibernating bears exhibit certain phenotypes
55 present in human disease, but importantly, these phenotypes do not themselves negatively impact
56 the bears' overall health [4-7]. For example, heart rate slows to 10 to 15 beats per minute [8], yet
57 bears do not develop typical dysfunction that would be characteristic of severe bradycardia in
58 humans. Bears prevent congestive heart failure or ventricular dilation by decreasing atrial
59 contractility and increasing atrial and ventricular stiffness [8, 9]. Hibernating bears are also well
60 known for maintaining muscle strength, morphology, and composition during hibernation in the
61 near complete absence of weight-bearing activity [10, 11]. Bears also exhibit insulin resistance
62 during hibernation but are insulin sensitive during the active season [7]. Although humans do not
63 hibernate, the unique metabolic adaptations that evolved in hibernators could provide clues to
64 develop new treatments for human metabolic diseases, such as obesity and type 2 diabetes [2]. In
65 fact, the need to accumulate tremendous amounts of fat and the development of insulin resistance
66 evolved in bears as a survival strategy [12-14]. Recent studies have shown that these hibernation-
67 induced physiological shifts are associated with massive changes in the regulation and
68 expression of thousands of genes across hibernation-relevant processes [15-17]. Notably, many
69 of these genes are involved in complex metabolic and cellular signaling pathways (e.g., insulin
70 signaling, metabolism) that play critical roles in a variety of biological processes across
71 vertebrates, including humans [15, 18].

72 Over ten thousand genes have been shown to be differentially regulated in adipose, liver, and
73 muscle tissues between active and hibernating states, providing a set of candidate genes involved
74 in the regulation of cellular and physiological processes that underly the metabolic suppression
75 observed in hibernation [15]. The genes identified represent key genes and genomic regions for
76 testing hypotheses related to the evolution and regulation of hibernation. While it is known that
77 mRNA isoforms vary between tissues, cell types, and developmental stages [19, 20] and play a
78 role in cellular processes, studies in bears have focused on global gene expression levels have not
79 investigated the mRNA processing shifts that result in different isoforms and thus proteome
80 output that occur with active and hibernating seasons.

81
82 We hypothesize that different transcript isoforms contribute to the reversible states
83 achieved during hibernation. Indeed, in brown bears and Himalayan black bears (*Ursus*
84 *thibetanus ussuricus*), it has been shown that the amount of titin does not differ between active
85 and hibernation seasons but the relative abundance of two prominent isoforms may explain
86 increased ventricular stiffness during hibernation [21, 22]. However, isoform differences have
87 been explored only in a few select cases and little is known about the role different isoforms
88 contribute to the hibernation phenotype on a large scale. Because of the capability of sequencing
89 full-length RNA transcripts, SMRT Sequencing is ideal for identifying the isoforms that are
90 differentially expressed between seasons. We compare full-length isoforms between hibernating
91 and active bears in three metabolically active tissues – skeletal muscle, liver, and adipose.

92



93

94 **Figure 1.** Bear transcriptome workflow. For each of the six bears, tissues (muscle, liver, adipose) were extracted
95 during active or hibernation seasons. PacBio Iso-Seq and Illumina RNA-seq data were collected from three of the
96 bears (orange) and Illumina RNA-seq data was collected from three additional bears (blue). Iso-Seq data was
97 processed through a pipeline of isoseq3, SQANTI3, and IsoAnnot, before merging with the reference transcriptome
98 to create a merged annotation set to map RNA-seq data using kallisto. Differential isoform expression and usage
99 was determined using tappAS.

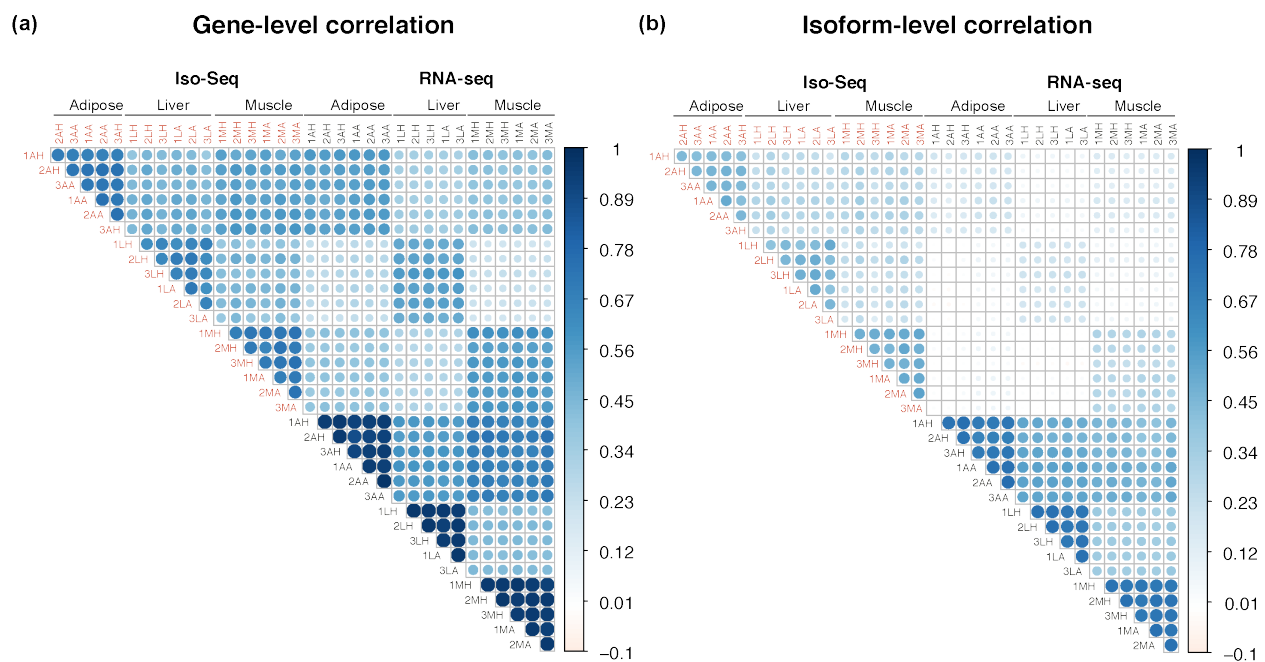
100

101 Results

102 High Correlation between Long- and Short-Read Data at Gene Level

103 We analyzed RNA-sequencing data from bears in active or hibernation seasons on three distinct
104 tissue types (muscle, adipose, liver). Three of the bears were sequenced using the PacBio Iso-Seq
105 protocol for full length RNA transcripts, and all six bears were sequenced using the short-read
106 Illumina RNA-seq approach (Figure 1). The RNA-seq data was previously analyzed in [15]. We
107 first combined all the long-read Iso-Seq data across samples and replicates and obtained a total
108 of 6.1 million full-length HiFi reads (Table S1). After running the HiFi reads through analysis,
109 mapping to the reference genome, and filtering for library artifacts, we obtained 76,071 unique,
110 full-length isoforms ranging from 150 basepairs (bp) to 16.5 kilobases (kb) (mean: 3.2 kb). We

111 then evaluated the gene-level correlation of long- versus short-read data. For this correlation, we
112 used only transcripts that were present in both Iso-Seq and RNA-seq datasets. When comparing
113 data from the same individuals (albeit sampled in different years), the highest correlations are
114 within data type, regardless of season (active or hibernation) (Figure 2). There is also a high
115 correlation between data types at the gene level, especially within the same tissues (Figure 2a).
116 The lower concordance at the isoform-level within the Iso-Seq samples as compared to the
117 within RNA-seq samples, is likely explained by the lower sequencing coverage of the long-read
118 dataset (Figure 2b). Nevertheless, we see consistent gene-level correlation for the matching
119 samples across data types, while samples from the same tissues or animals have higher
120 correlation than different tissues, as expected.



121
122 **Figure 2.** Gene- and isoform-level correlation between Iso-Seq and RNA-seq count data (log counts per
123 million). Correlation measured with Pearson correlation. Samples are coded using three letters representing
124 [animal], [tissue], and [season]. The three bears were numbered. The tissues were adipose (A), liver (L), and
125 muscle (M). The seasons were hibernation (H) or active (A).

126

127 **An Improved Reference Transcriptome and Full-Length Isoform Annotation using Iso-Seq**

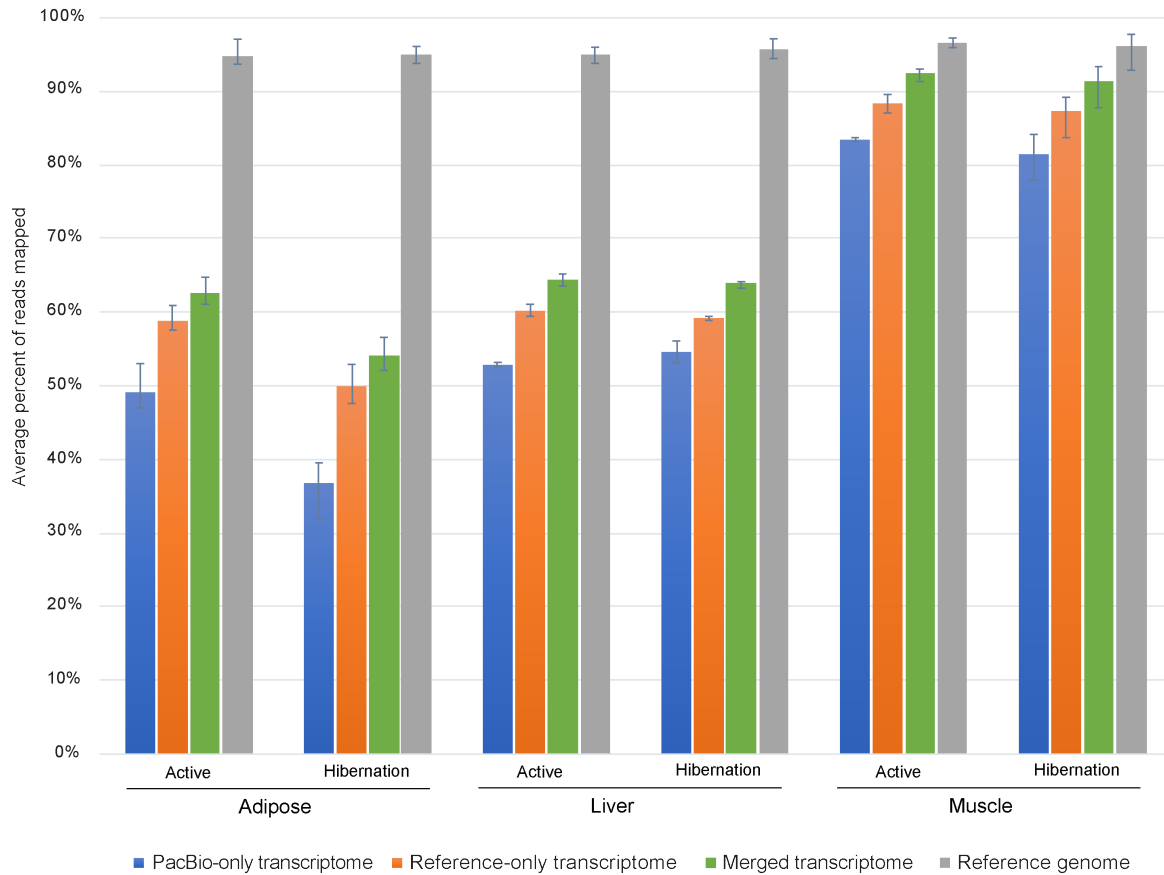
128 The existing reference transcriptome contained 30,263 genes encompassing 58,335 transcripts.
129 The Iso-Seq transcriptome was classified against the reference transcriptome and found to
130 contain 12,018 known and 907 novel genes (Table S2). Compared with the reference annotation,
131 27.8% of the Iso-Seq isoforms were categorized as full-splice matches (FSMs; perfect matches to
132 a reference transcript), while over half of the isoforms were novel isoforms (NIC, novel in
133 catalog or NNC, novel not in catalog). More than 30% of the genes had complex splicing events
134 (greater than six isoforms). Novel isoforms had a higher proportion of having a predicted
135 nonsense mediated decay (NMD) effect (see the left panel of Figure S1a-S1d).

136
137 We merged the existing reference transcriptome with the new Iso-Seq transcriptome data,
138 resulting in a total of 31,829 genes encompassing 107,649 transcripts. The merged data set had a
139 reduced number of incomplete splice matches (ISM) and novel isoforms (NIC, NNC) while
140 greatly increasing the number of known transcripts (Table S3), suggesting a more comprehensive
141 representation of the transcriptome. When analyzing transcripts expressed in each tissue, by
142 mapping RNA-seq data from six bears, we found that each tissue (muscle, liver, adipose) had
143 different distributions of transcript structural changes, with adipose and liver having similar
144 distributions and muscle having a much larger number of full-splice match (FSM) and fewer
145 novel in catalog (NIC) transcripts (Figure S2). Importantly, the improved reference
146 transcriptome, with the full-length transcripts originating from samples of interest, provides a
147 starting point for the discovery of differential isoform usage (DIU) that would otherwise be
148 missed. One example of such a finding is the isoform expression of the *CA2* gene (Figure S1e),
149 described in more detail in later sections.

150

151 To evaluate the degree to which the Iso-Seq dataset captures the expressed transcripts in the
152 tissues of interest, we mapped the ribosomal RNA-depleted (Ribo-Zero) short-read RNA-seq
153 data of the same tissues (adipose, liver, muscle) and seasons (active and hibernation) to either a
154 PacBio-only transcriptome, the reference-only transcriptome, a PacBio-reference merged
155 transcriptome, or the reference genome (Figure 3). Given the lower sequencing depth of the
156 PacBio data, we were not surprised to see a higher mappability of the short reads to the reference
157 transcriptome than to the PacBio-only transcriptome. However, the merged PacBio-reference
158 transcriptome showed the highest mappability of all transcriptomes. Of note, in the adipose and
159 liver tissues, a higher proportion of intronic reads in the ribosomal-depleted RNA-seq data
160 resulted in a much higher mappability using the reference genome. With the demonstrated
161 improvement of the transcriptome by adding the Iso-Seq data, the merged (PacBio and reference)
162 transcriptome was used for further analyses.

163



164

165 **Figure 3.** Ribosomal RNA depleted RNA-seq data mapped to transcriptomes and the reference genome.

166 Average percent of reads mapped per season and tissue. Error bars indicate range.

167

168 **Tissue-specific Differential Isoform Usage from Active to Hibernation Season**

169

170 We assessed whether the relative abundance of different isoforms for each gene varied between

171 the seasons (differential isoform usage, DIU). We also determined whether the major (highest

172 expressed) isoform switched between seasons. When analyzing for DIU and major isoform

173 switching between the seasons (hibernation vs active), there were substantial differences among

174 the tissues (Table 1, Figure S3). Adipose had the highest incidence of DIU with regards to both

175 number and percent of all analyzed genes, with and without major isoform switching (27.5% of
176 genes; Table 1). In contrast, major isoform switching between states without differential isoform
177 usage was fairly consistent across tissues.

	Adipose	Liver	Muscle
DIU – Major Isoform Switching	779 (8.7%)	201 (2.7%)	85 (1.6%)
DIU – No Major Isoform Switching	1679 (18.8%)	379 (5.0%)	198 (3.7%)
Not DIU – Major Isoform Switching	1196 (13.4%)	1228 (16.3%)	826 (15.4%)
Not DIU – No Major Isoform Switching	5268 (59.0%)	5706 (75.9%)	4255 (79.3%)
Total Genes Analyzed	8922	7514	5364

178
179 **Table 1:** Number and percentage of genes showing differential isoform usage (DIU) and/or major isoform
180 switching between hibernation and active seasons in each tissue.

181 182 **Isoform Switching between Active and Hibernation Seasons Despite No Gene-Level**

183 **Expression Change**

184 In this study and in prior work, gene expression changes were detected in all three tissues
185 between active and hibernating seasons. With the new isoform-level quantifications, we
186 examined whether the genes classified as having both DIU and Major Isoform Switching
187 between the two seasons (Table 1) were enriched in specific cellular functions. Of the three
188 tissues, adipose displayed the most DIU + Major Isoform switches between seasons, with the
189 encoded genes displaying enrichment for biosynthetic and metabolic processes (Table S4). We
190 then restricted the list of DIU and Major Isoform switching genes to those that displayed less
191 than 20% change in overall gene-level expression in response to the season. Testing this list of
192 genes for enrichments in cellular function found a shift to more modest enrichments with the top
193 categories focused on autophagy (Table S5). This indicates that one component of hibernation

194 adaptations, the need to consume reserve fat stores, is partly re-programmed by a shift in mRNA
195 isoform ratios rather than the overall expression level of the gene.

196

197 One gene that shows a dramatic isoform switch in adipose in concert with the seasons is Integrin

198 Subunit Beta 3 Binding Protein (*ITGB3BP*), imparting a nearly binary switch in five of the six

199 sampled bears (Figure 4). There is very little change in overall gene expression but the major

200 isoform switches between active and hibernation (Figure 4a, b). The two isoforms differ by a

201 cassette exon near the 3' end of the open reading frame, resulting in a new C-terminal peptide

202 sequence for the protein. Prior characterization of the *ITGB3BP* protein in mammals

203 demonstrated that it acts as transcriptional co-regulator amongst several nuclear hormone

204 receptor circuits affecting both the retinoic acid (RXR) and thyroid hormone (TR) pathways.

205 Since nuclear hormones play a key role in metabolic control and are implicated in homeostasis

206 during hibernation, we further investigated the putative consequences of the isoform switch [23].

207 The bear isoform PB.6860.1, which is predominant in bear adipose tissue during hibernation,

208 includes a cassette exon near the 3' end of the open reading frame and encodes a protein isoform

209 of the same 177 amino acid length as the predominant human isoform with 76% identity (Figure

210 4d). Skipping of the cassette exon (PB.6860.2) is more common during the active season, and

211 this splicing pattern is also observed in humans, according to GTEx project data [24]. This event

212 results in a truncated C-terminus, which we predict would alter the downstream co-regulator

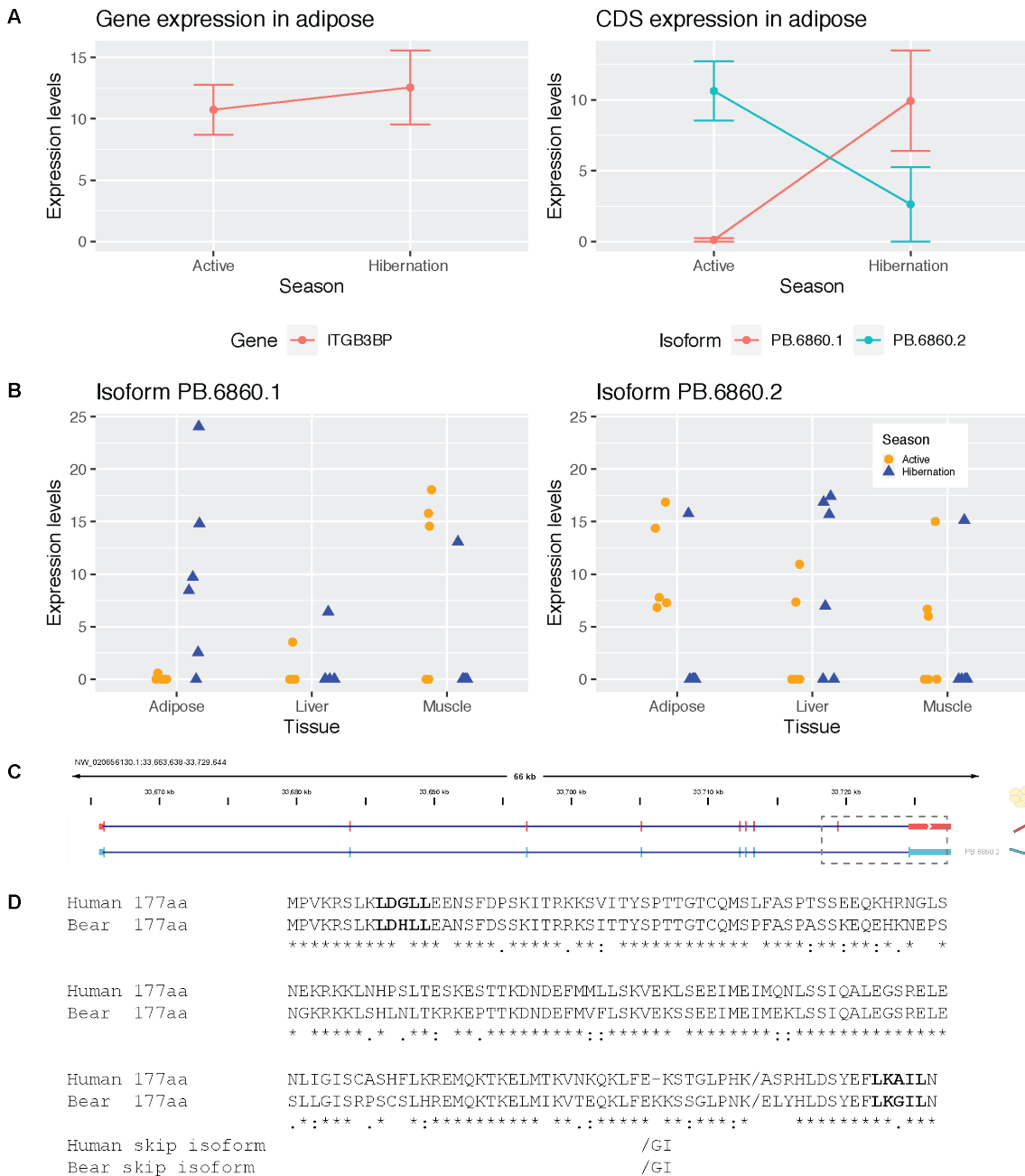
213 activity of *ITGB3BP* based on studies of its domain structure. Studies of the human protein

214 showed that the C-terminal LXXIL motif, conserved in the bear and encoded by the exon-

215 included isoform (PB.6860.1), acts as a receptor-interaction domain (RID) [25]. This motif along

216 with the human N-terminal LXXLL motif, also conserved in the bear, act in a cooperative

217 fashion during interaction with the nuclear hormone receptor dimer. As the isoform without the
218 exon (PB.6860.2) lacks the C-terminal LXXIL motif and terminates instead with a dipeptide GI,
219 this alternative splicing event may impart broad downstream consequences for hormone receptor
220 signaling in adipose tissue while bears are in an active state.



221

222 **Figure 4.** Differential isoform expression of *ITGB3BP* mRNA in adipose tissue. (a) expression changes at the
 223 gene and coding sequence (CDS) level. (b) Short read expression of the two *ITGB3BP* isoforms across all
 224 bears and tissues. (c) Isoform structure of two *ITGB3BP* isoforms, dashed box indicates the region of the
 225 isoforms that differs. (d) Protein alignment (MUSCLE) for the human isoform and the bear isoform observed

226 in the active season. Putative functional motifs based on the human protein co-activator function are shown in
227 larger bold text. The bold slash represents the beginning of C-terminal peptide sequence altered by the splicing
228 event observed in hibernating bears. The skipped exon results in a shorter C-terminus shown below the full-
229 length alignments.

230

231 In liver, an example of a gene with significant DIU and isoform switching was Carbonic
232 Anhydrase 2 (*CA2*). The *CA2* gene expressed two isoforms (Figure S4). The shorter isoform,
233 which lacks a coding exon and initiates transcription downstream compared to the other isoform,
234 was upregulated in the hibernation season for all six bears, while the longer isoform showed
235 decreased expression during hibernation. Interestingly, the shorter isoform, which is annotated in
236 the human genome, was not annotated in the reference transcriptome and was only found in the
237 PacBio Iso-Seq data (Figure S1e).

238

239 In muscle, an example of a gene with significant DIU and isoform switching, was cryptochrome
240 2 (*CRY2*). There are four expressed isoforms of *CRY2*, two of which are novel and showed very
241 little changes from active season to hibernation and the other two isoforms, which show major
242 isoform switching (Figure S5). The two isoforms that show major isoform switching differed by
243 only 14 bp at the last donor site; both isoforms were annotated in the reference, and both were
244 predicted to encode for the same protein. The longer isoform showed decreased isoform usage
245 while the shorter isoform showed increased isoform usage during hibernation.

246

247 In addition to identifying genes with DIU and major isoform switching, we also identified genes
248 with evidence for DIU without major isoform switching (Table 1). For example, four transcript
249 isoforms of the homeobox transcription factor *PRRX1* (Figure S6), corresponding to human

250 *PRRX1a* (PB.14470.3); *PRRX1b* (PB.14470.1), and an unnamed human isoform (PB.14470.4).
251 The fourth transcript, PB.14470.2, is a non-coding isoform. Transcription factor *PRRX1* is highly
252 expressed in adipose and muscle. In adipose, the PB.14470.1 isoform continues to predominate
253 in both active and hibernation seasons compared to the other isoforms, but also shows
254 significantly higher expression during hibernation. This isoform (PB.14470.1) also contains a
255 3280 bp 5' UTR that is lacking in PB.14470.3 while the latter contains a fifth exon. This same
256 transcription factor in muscle shows no change in isoform expression between the seasons
257 (Figure S6).

258
259 A gene that shows DIU and is positively regulated in adipose by *PRRX1* in humans is *COL6A3*.
260 *COL6A3* expression is positively related to *PRRX1* in hibernation, but not in active season
261 adipose (Figure S7); overall the relationship between these two genes is opposite to that in
262 humans. Two coding isoforms (out of six) of *COL6A3* predominate and both isoforms are
263 reduced in hibernation compared to active season (Figure S7).

264
265

266 **Discussion**

267 Our study provides an unprecedented view into hibernation biology through the lens of RNA
268 processing by producing a dataset that improved the annotation of the brown bear genome and
269 reinforced the important role adipose tissue plays in hibernation. This approach allowed us to
270 characterize isoforms that are changing between active and hibernation states, even when the
271 gene itself shows no significant change in expression levels. While studies of differentially
272 expressed genes have provided much of our current understanding in hibernation biology [15,

273 26-31], determining genes where functionally distinct isoforms change between seasons is the
274 next essential biological mechanism to uncover.

275
276 As we have shown in this study, metabolically active tissues vary dramatically in their isoform
277 usage. The inherent complexity and importance of adipose, which has been recognized as a
278 source of critical physiological mechanisms during hibernation [7, 15], continues to expand. The
279 large percentage of genes with DIU compared to liver and muscle, and the large number of
280 differentially expressed genes support the dynamic role of adipose in hibernation where both
281 transcription and RNA processing play concerted roles. The difference in the percentage of reads
282 mapping to the transcriptome as compared to the genome in adipose and liver suggests that the
283 ribosomal-depleted RNA-seq data had more intronic and intergenic reads in those tissues. It is
284 also important to note that slightly different extraction kits were used for the muscle as compared
285 to adipose and liver tissue RNA extraction for the short-read data [15]. While extraction method
286 may influence the percentage of intronic and intergenic reads, there may also be differences in
287 splicing efficiency between tissues and states. Regardless, adipose showed differences between
288 active and hibernation, suggesting that intron retention may be an especially important
289 mechanism for gene regulation and function in adipose during hibernation. It is also possible that
290 global rates and efficiency of RNA processing by the spliceosome may also vary between the
291 tissues and states.

292
293 In addition to hibernation biology, our results also highlight several transcriptional events that
294 may have important implications for humans. For example, the very strong positive relationship
295 between *COL6A3* and *PRXX1* expression in human adipose tissue [32] is completely absent in

296 bears, providing a possible explanation for why bears exhibit little to no inflammatory signatures
297 even during periods of extreme adiposity and when consuming a high saturated fat diet
298 [33]. Even the expected (positive) relationship between *COL6A3* and TGF β is absent in bears.
299 However, elevated PRRX1 is associated with PPARG (Peroxisome Proliferator Activated
300 Receptor Gamma) reductions in hibernation bear adipose tissue as has been observed previously
301 [34]. Thus, certain aspects of adipose function appear dissociable in bears which could lead to a
302 more precise understanding of the contribution of adipose tissue to human disease states.
303 Furthermore, since various single nucleotide polymorphisms within the homeobox domain
304 superfamily associate with type 2 diabetes in humans, manipulation of PRRX1 isoforms in
305 hibernation bear adipocytes (insulin resistant) *in vitro* could be used to test these relationships
306 more precisely without the confounding interaction with COL6A3.

307
308 While PacBio Iso-Seq has been used widely for plant and animal genome annotation [35, 36],
309 and recently shown to shed light in cell-type specific isoform expressions in brain regions [37],
310 this study included multiple biological replicates per tissue and condition that incorporated both
311 RNA-seq and Iso-Seq data for identifying differential isoform usage. The high mappability of the
312 matching RNA-seq data to the Iso-Seq transcriptome shows promise for other less well-
313 annotated organisms, where Iso-Seq may serve as a sole reference transcriptome upon which
314 RNA-seq may be used for differential analysis. We saw a high correlation at the gene level
315 between data types from the same tissue despite the fact that the Iso-Seq data were lower
316 coverage. There was also a moderate correlation at the isoform level within data type, but less so
317 between data types, likely because of the low sequencing depth of the long-read data.

318

319 Moving forward, we aim to create an improved reference transcriptome at higher coverage, as
320 well as improve the existing reference genome, to create a comprehensive reference that may
321 better serve for studying differential isoform expressions in hibernation. Comparative studies
322 across bears will also provide a much-needed framework for comparing hibernating and non-
323 hibernating species. Indeed, long-read sequencing was used to improve the polar bear reference
324 genome annotation set [38], which provides a valuable additional resource for comparative
325 studies. Although the *U. arctos* genome [39] is not a chromosome-level assembly, we were able
326 to improve the annotations and these data can be used in future improvements of the genome
327 assembly.

328

329 In summary, our study demonstrates the utility of PacBio Iso-Seq for determining isoform
330 differences between hibernating and active brown bears. Importantly, we found that adipose is
331 the most dynamic tissue during hibernation with the highest number of genes with differential
332 isoform usage and isoform switching as compared to liver and muscle. These findings and
333 datasets provide a rich new resource for studying hibernation biology and understanding
334 metabolic function. Additionally, this resource provides a basis for incorporating isoform
335 changes in studying hibernation and translating findings to solving human diseases.

336

337 **Methods**

338 **Sample Collection**

339 For the PacBio Iso-Seq protocol, samples were collected from three bears (1 female, 2
340 males) at the Washington State University Bear Research, Education, and Conservation Center in
341 January 2019 and May 2019, to represent the winter hibernation and summer active periods,
342 respectively. Muscle, liver, and adipose tissue samples were collected for a total of 18 samples.
343 Samples for the Illumina Ribo-Zero RNA-seq data were collected in May 2015 and January 2016
344 and are described in detail in [15]. Animal care details are described in [7]. Bears were first
345 anesthetized using the protocol described in Ware JV, Nelson OL, Robbins CT and Jansen HT
346 [40]. Subcutaneous adipose samples were collected using a 6mm punch biopsy (Miltex, York,
347 PA) as described in [7], while skeletal muscle (gastrocnemius) and liver tissue samples were
348 collected with a 14G tru-cut biopsy needle (Progressive Medical International, Vista, CA, USA).
349 All samples were collected between 0800 and 1200hr. Samples were immediately flash frozen in
350 liquid nitrogen and transferred to a -80°C freezer, where they were stored until shipment to the
351 University of Delaware Sequencing & Genotyping Center for RNA extraction. Procedures for all
352 experiments were approved by the Institutional Animal Care and Use Committee at Washington
353 State University (Protocol #04922).

354

355 **PacBio Iso-Seq Library Preparation and Sequencing**

356 Total RNAs were extracted from tissue samples and isolated using the RNeasy Universal kit
357 (Qiagen, Valencia, CA, USA) as per the manufacturer's standard protocol. Following total RNA
358 isolation, the samples were concentrated using RNA Clean & Concentrator Kit (Zymo Research,
359 Irvine CA, USA). The purity of RNA samples was measured using the DeNovix DS-11+

360 spectrophotometer (DeNovix Inc., Wilmington, DE, USA). RNA concentration was measured
361 using Qubit High Sensitivity RNA Assay Kit and Qubit 3.0 Fluorometer (Thermo Fisher
362 Scientific Inc., Waltham, MA, USA). The integrity of total RNA was assessed on the Agilent
363 Fragment Analyzer 5200 system (Agilent Technologies, Santa Clara, CA, USA) using the High
364 Sensitivity RNA Kit. The RNA Quality Number (RQN) criteria for the RNA samples was RQN
365 >7.0.

366

367 From 100ng to 300ng of total RNA was input for cDNA synthesis and amplification using
368 NEBNext Single Cell/Low Input cDNA Synthesis & Amplification Module (New England
369 BioLabs Inc., Ipswich, MA, USA) as per the manufacturer's standard protocol. This is a poly-A
370 selection library preparation method. A total of 10-15 PCR cycles were used to generate
371 sufficient quantities of cDNA for PacBio Iso-Seq library preparations. Concentration and size
372 profile of cDNA samples was assessed on the Agilent Fragment Analyzer 5200 system (Agilent
373 Technologies, Santa Clara, CA, USA) using the High Sensitivity Large Fragment Kit.

374

375 Amplified cDNA samples were size selected using ProNex Size-Selective Purification System
376 (Promega Corporation, Madison, WI, USA) as per the PacBio recommendation for standard
377 length cDNA transcripts. Size selected cDNA was used to construct SMRTbell Iso-Seq libraries
378 using Express Template Prep 2.0 (Pacific Biosciences, Menlo Park, CA, USA) as per the
379 manufacturer's Iso-Seq Express Template Preparation protocol. The concentration of the Iso-Seq
380 libraries was measured using the Qubit 3.0 Fluorometer (Thermo Fisher Scientific Inc.,
381 Waltham, MA, USA). The fragment size profile of the Iso-Seq libraries was assessed on the
382 (Agilent Technologies, Santa Clara, CA, USA). Each Iso-Seq library was run on a single Sequel

383 system SMRT Cell using sequencing chemistry 3.0 with 4 hour pre-extension and 20 hour movie
384 time. One SMRT Cell per tissue and state was used to provide deep coverage of the entire grizzly
385 transcriptome. Raw reads were processed into circular consensus sequence (CCS) reads as per
386 the manufacturer's standard pipeline (SMRT Link version 7.0).

387

388 **PacBio Iso-Seq Bioinformatic Analysis**

389 All 18 SMRT Cells of Iso-Seq data from different samples were pooled and run through the
390 IsoSeq Analysis in SMRTLink v8.1 which generated full-length, high-quality (HQ) isoform
391 sequences. The HQ isoforms were mapped to the genome assembly (GCA_003584765.1) using
392 minimap2, then filtered and collapsed into non-redundant isoforms using Cupcake following the
393 analysis described at ([https://github.com/Magdoll/cDNA_Cupcake/wiki/Cupcake:-supporting-](https://github.com/Magdoll/cDNA_Cupcake/wiki/Cupcake:-supporting-scripts-for-Iso-Seq-after-clustering-step)
394 [scripts-for-Iso-Seq-after-clustering-step](https://github.com/Magdoll/cDNA_Cupcake/wiki/Cupcake:-supporting-scripts-for-Iso-Seq-after-clustering-step)). The non-redundant isoforms were then classified
395 against the GCA_003584765.1 reference transcriptome using SQANTI3
396 (<https://github.com/ConesaLab/SQANTI3>). After running SQANTI3 classification and filtering,
397 we obtained a final set of PacBio isoforms that we used subsequently as the reference
398 transcriptome for short read quantification. As part of the Cupcake processing pipeline, we
399 obtained full-length read counts associated with each isoform, which were then normalized into
400 Full-Length Counts Per Million (CPM) for cross-sample comparison.

401

402 **Short-read RNA-seq Quantification**

403 Short-read Illumina data from [15] for the same individuals and tissues, sampled in a different
404 year, were mapped to the final set of PacBio isoforms using the kallisto quantification algorithm,

405 with the rf-stranded flag [43]. Read counts were compared to the IsoSeq data using Pearson
406 correlation on the \log_2 count per million.

407

408 **Merging annotations and mapping**

409 The PacBio-only annotation set was merged with the reference-only annotations using
410 gffcompare [41]. Short read Illumina data from [15] was mapped to each transcriptome and the
411 reference genome (GenBank assembly accession: GCA_003584765.1 [39]) using HISAT2
412 (version 2.2.1) with the --rf flag and otherwise default parameters [42].

413

414 **Functional Annotation and Differential Isoform Expression Analysis**

415 Abundance count estimates for each individual were combined into a single input matrix for
416 tappAS [44]. The annotation file generated in SQANTI3 and the short-read count matrices for
417 each tissue were input into tappAS [44]. Each tissue was analyzed separately to compare
418 differential isoform expression in hibernation compared to active season. We excluded short-read
419 data from sample 1AA because it was previously shown to contain a hair follicle [15].

420 Transcripts with counts per million (cpm) less than 1.0 or coefficient of variation cutoff of 100%

421 were excluded from the analyses. In the differential isoform usage (DIU) analysis, minor

422 isoforms with a proportional of expression difference less than 0.1 were excluded from the

423 analysis and DIU was considered at an FDR < 0.05. Gene ontology (GO) enrichment of different

424 gene sets was calculated using PANTHER [45] with the following parameters: Analysis

425 Type: PANTHER Overrepresentation Test (Released 20210224), Annotation Version and

426 Release Date: GO Ontology database DOI: 10.5281/zenodo.4495804 Released 2021-02-01,

427 Reference List: Homo sapiens (all genes in database), Annotation Data Set: GO biological
428 process, Test Type: Fisher's Exact, Correction: Calculate False Discovery Rate.
429

430 **Declarations**

431 **Ethics Approval and Consent to Participate**

432 The bears used in this study were housed at the Washington State University Bear Research,
433 Education, and Conservation Center. All procedures were approved by the Washington State
434 University Institutional Animal Care and Use Committee (IACUC) under protocol number
435 ASAF 6546.

436

437 **Availability of Data and Materials**

438 The datasets generated for the current study are available in the NCBI SRA repository under
439 BioProject PRJNA727613. The datasets reanalyzed in this study are available in the NCBI SRA
440 repository under BioProject PRJNA413091. The code for this project is available at:
441 <https://github.com/jokelley/brownbear-iseq-act-hib>

442

443 **Competing Interests**

444 Elizabeth Tseng, Jason G. Underwood and Michelle Vierra are employees of Pacific
445 Biosciences.

446

447 **Funding**

448 The sequencing for this project was funded by a Pacific Biosciences (PacBio) SMRT grant.
449 We would also like to acknowledge the Interagency Grizzly Bear Committee, USDA National
450 Institute of Food and Agriculture (McIntire-Stennis project 1018967), International Association
451 for Bear Research and Management, T. N. Tollefson and Mazuri Exotic Animal Nutrition, the

452 Raili Korkka Brown Bear Endowment, Nutritional Ecology Endowment, and Bear Research and
453 Conservation Endowment at Washington State University for funding and support.

454

455 **Authors' Contributions**

456 BDEH, ST, BK, MV, CTR, HTJ, JLK contributed to sampling. BK, OS, and EB performed the
457 RNA extraction, library preparation, and sequencing. JGU, MV, and HTJ contributed to the
458 manuscript. ET and JLK analyzed the data and wrote the manuscript. All authors read and
459 approved the final manuscript.

460

461 **Acknowledgements**

462 This research used resources from the Center for Institutional Research Computing at
463 Washington State University. Allan Cornejo Kelley for feedback on figures.

464

465 References

- 466 1. Stenvinkel P, Jani AH, Johnson RJ: **Hibernating bears (Ursidae): metabolic magicians**
467 **of definite interest for the nephrologist.** *Kidney Int* 2013, **83**:207-212.
- 468 2. Martin SL: **Mammalian hibernation: a naturally reversible model for insulin**
469 **resistance in man?** *Diab Vasc Dis Res* 2008, **5**:76-81.
- 470 3. Hellgren EC: **Physiology of hibernation in bears.** *Ursus, Vol 10 - 1998* 1998, **10**:467-
471 477.
- 472 4. Berg von Linde M, Arevstrom L, Frobert O: **Insights from the Den: How Hibernating**
473 **Bears May Help Us Understand and Treat Human Disease.** *Clin Transl Sci* 2015,
474 **8**:601-605.
- 475 5. Welinder KG, Hansen R, Overgaard MT, Brohus M, Sonderkaer M, von Bergen M,
476 Rolle-Kampczyk U, Otto W, Lindahl TL, Arinell K, et al: **Biochemical Foundations of**
477 **Health and Energy Conservation in Hibernating Free-ranging Subadult Brown**
478 **Bear Ursus arctos.** *Journal of Biological Chemistry* 2016, **291**:22509-22523.
- 479 6. Fedorov VB, Goropashnaya AV, Toien O, Stewart NC, Gracey AY, Chang CL, Qin SZ,
480 Pertea G, Quackenbush J, Showe LC, et al: **Elevated expression of protein biosynthesis**
481 **genes in liver and muscle of hibernating black bears (Ursus americanus).**
482 *Physiological Genomics* 2009, **37**:108-118.
- 483 7. Rigano KS, Gehring JL, Evans Hutzenbiler BD, Chen AV, Nelson OL, Vella CA,
484 Robbins CT, Jansen HT: **Life in the fat lane: seasonal regulation of insulin sensitivity,**
485 **food intake, and adipose biology in brown bears.** *J Comp Physiol B* 2017, **187**:649-
486 676.
- 487 8. Nelson OL, Robbins CT: **Cardiac function adaptations in hibernating grizzly bears**
488 **(Ursus arctos horribilis).** *Journal of Comparative Physiology B-Biochemical Systemic*
489 *and Environmental Physiology* 2010, **180**:465-473.
- 490 9. Barrows ND, Nelson OL, Robbins CT, Rourke BC: **Increased Cardiac Alpha-Myosin**
491 **Heavy Chain in Left Atria and Decreased Myocardial Insulin-Like Growth Factor**
492 **(IGF-I) Expression Accompany Low Heart Rate in Hibernating Grizzly Bears.**
493 *Physiological and Biochemical Zoology* 2011, **84**:1-17.
- 494 10. Harlow HJ, Lohuis T, Beck TD, Iaizzo PA: **Muscle strength in overwintering bears.**
495 *Nature* 2001, **409**:997.
- 496 11. Hershey JD, Robbins CT, Nelson OL, Lin DC: **Minimal seasonal alterations in the**
497 **skeletal muscle of captive brown bears.** *Physiological and Biochemical Zoology* 2008,
498 **81**:138-147.
- 499 12. Nelson R, Jones J, Wahner H, McGill D, Code C: **Nitrogen metabolism in bears: urea**
500 **metabolism in summer starvation and in winter sleep and role of urinary bladder in**
501 **water and nitrogen conservation.** In *Mayo Clinic Proceedings.* 1975: 141-146.
- 502 13. Nelson RA, Wahner HW, Jones JD, Ellefson RD, Zollman PE: **Metabolism of bears**
503 **before, during, and after winter sleep.** *Am J Physiol* 1973, **224**:491-496.
- 504 14. Palumbo PJ, Wellik DL, Bagley NA, Nelson RA: **Insulin and Glucagon Responses in**
505 **the Hibernating Black Bear.** *Bears: Their Biology and Management* 1983, **5**:291-296.
- 506 15. Jansen HT, Trojahn S, Saxton MW, Quackenbush CR, Evans Hutzenbiler BD, Nelson
507 OL, Cornejo OE, Robbins CT, Kelley JL: **Hibernation induces widespread**
508 **transcriptional remodeling in metabolic tissues of the grizzly bear.** *Commun Biol*
509 2019, **2**:336.

- 510 16. Fedorov VB, Goropashnaya AV, Stewart NC, Tøien Ø, Chang C, Wang H, Yan J, Showe
511 LC, Showe MK, Barnes BM: **Comparative functional genomics of adaptation to**
512 **muscular disuse in hibernating mammals.** *Molecular ecology* 2014, **23**:5524-5537.
- 513 17. Fedorov VB, Goropashnaya AV, Toien O, Stewart NC, Chang C, Wang HF, Yan J,
514 Showe LC, Showe MK, Barnes BM: **Modulation of gene expression in heart and liver**
515 **of hibernating black bears (*Ursus americanus*).** *Bmc Genomics* 2011, **12**.
- 516 18. Cheatham B, Kahn CR: **Insulin action and the insulin signaling network.** *Endocr Rev*
517 1995, **16**:117-142.
- 518 19. Wang ET, Sandberg R, Luo S, Khrebtkova I, Zhang L, Mayr C, Kingsmore SF, Schroth
519 GP, Burge CB: **Alternative isoform regulation in human tissue transcriptomes.**
520 *Nature* 2008, **456**:470-476.
- 521 20. Zhang X, Chen MH, Wu X, Kodani A, Fan J, Doan R, Ozawa M, Ma J, Yoshida N,
522 Reiter JF, et al: **Cell-Type-Specific Alternative Splicing Governs Cell Fate in the**
523 **Developing Cerebral Cortex.** *Cell* 2016, **166**:1147-1162 e1115.
- 524 21. Nelson OL, Robbins CT, Wu YM, Granzier H: **Titin isoform switching is a major**
525 **cardiac adaptive response in hibernating grizzly bears.** *American Journal of*
526 *Physiology-Heart and Circulatory Physiology* 2008, **295**:H366-H371.
- 527 22. Salmov N, Vikhlyantsev I, Ulanova A, Gritsyna Y, Bobylev A, Saveljev A,
528 Makariushchenko V, Maksudov G, Podlubnaya Z: **Seasonal changes in isoform**
529 **composition of giant proteins of thick and thin filaments and titin (connectin)**
530 **phosphorylation level in striated muscles of bears (*Ursidae*, *Mammalia*).**
531 *Biochemistry (Moscow)* 2015, **80**:343-355.
- 532 23. Nelson CJ, Otis JP, Carey HV: **A role for nuclear receptors in mammalian**
533 **hibernation.** *J Physiol* 2009, **587**:1863-1870.
- 534 24. Aguet F, Brown AA, Castel SE, Davis JR, He Y, Jo B, Mohammadi P, Park Y, Parsana
535 P, Segrè AV, et al: **Genetic effects on gene expression across human tissues.** *Nature*
536 2017, **550**:204-213.
- 537 25. Li D, Wang F, Samuels HH: **Domain structure of the NRIF3 family of coregulators**
538 **suggests potential dual roles in transcriptional regulation.** *Mol Cell Biol* 2001,
539 **21**:8371-8384.
- 540 26. Chayama Y, Ando L, Sato Y, Shigenobu S, Anegawa D, Fujimoto T, Taii H, Tamura Y,
541 Miura M, Yamaguchi Y: **Molecular Basis of White Adipose Tissue Remodeling That**
542 **Precedes and Coincides With Hibernation in the Syrian Hamster, a Food-Storing**
543 **Hibernator.** *Front Physiol* 2018, **9**:1973.
- 544 27. Srivastava A, Kumar Sarsani V, Fiddes I, Sheehan SM, Seger RL, Barter ME, Neptune-
545 Bear S, Lindqvist C, Korstanje R: **Genome assembly and gene expression in the**
546 **American black bear provides new insights into the renal response to hibernation.**
547 *DNA Res* 2019, **26**:37-44.
- 548 28. Sreere HK, Wang LCH, Martin SL: **Central Role for Differential Gene-Expression in**
549 **Mammalian Hibernation.** *Proceedings of the National Academy of Sciences of the*
550 *United States of America* 1992, **89**:7119-7123.
- 551 29. Shimozuru M, Nagashima A, Tanaka J, Tsubota T: **Seasonal changes in the expression**
552 **of energy metabolism-related genes in white adipose tissue and skeletal muscle in**
553 **female Japanese black bears.** *Comparative Biochemistry and Physiology B-*
554 *Biochemistry & Molecular Biology* 2016, **196**:38-47.

- 555 30. Gautier C, Bothorel B, Ciocca D, Valour D, Gaudeau A, Dupré C, Lizzo G, Brasseur C,
556 Riest-Fery I, Stephan J-P, et al: **Gene expression profiling during hibernation in the**
557 **European hamster.** *Scientific Reports* 2018, **8**:13167.
- 558 31. Faherty SL, Villanueva-Canas JL, Blanco MB, Alba MM, Yoder AD: **Transcriptomics**
559 **in the wild: Hibernation physiology in free-ranging dwarf lemurs.** *Mol Ecol* 2018,
560 **27**:709-722.
- 561 32. Dankel SN, Grytten E, Bjune JI, Nielsen HJ, Dietrich A, Bluhner M, Sagen JV, Mellgren
562 G: **COL6A3 expression in adipose tissue cells is associated with levels of the**
563 **homeobox transcription factor PRRX1.** *Sci Rep* 2020, **10**:20164.
- 564 33. Rivet DR, Nelson OL, Vella CA, Jansen HT, Robbins CT: **Systemic effects of a high**
565 **saturated fat diet in grizzly bears (*Ursus arctos horribilis*).** *Canadian Journal of*
566 *Zoology* 2017, **95**:797-807.
- 567 34. Claussnitzer M, Dankel SN, Klocke B, Grallert H, Glunk V, Berulava T, Lee H,
568 Oskolkov N, Fadista J, Ehlers K, et al: **Leveraging cross-species transcription factor**
569 **binding site patterns: from diabetes risk loci to disease mechanisms.** *Cell* 2014,
570 **156**:343-358.
- 571 35. Wang B, Tseng E, Baybayan P, Eng K, Regulski M, Jiao Y, Wang L, Olson A, Chougule
572 K, Buren PV, Ware D: **Variant phasing and haplotypic expression from long-read**
573 **sequencing in maize.** *Communications Biology* 2020, **3**:78.
- 574 36. Ramberg S, Hoyheim B, Ostbye TK, Andreassen R: **A de novo Full-Length mRNA**
575 **Transcriptome Generated From Hybrid-Corrected PacBio Long-Reads Improves**
576 **the Transcript Annotation and Identifies Thousands of Novel Splice Variants in**
577 **Atlantic Salmon.** *Front Genet* 2021, **12**:656334.
- 578 37. Gupta I, Collier PG, Haase B, Mahfouz A, Joglekar A, Floyd T, Koopmans F, Barres B,
579 Smit AB, Sloan SA, et al: **Single-cell isoform RNA sequencing characterizes isoforms**
580 **in thousands of cerebellar cells.** *Nat Biotechnol* 2018.
- 581 38. Byrne A, Supple MA, Volden R, Laidre KL, Shapiro B, Vollmers C: **Depletion of**
582 **Hemoglobin Transcripts and Long-Read Sequencing Improves the Transcriptome**
583 **Annotation of the Polar Bear (*Ursus maritimus*).** *Frontiers in Genetics* 2019, **10**.
- 584 39. Taylor GA, Kirk H, Coombe L, Jackman SD, Chu J, Tse K, Cheng D, Chuah E, Pandoh
585 P, Carlsen R, et al: **The Genome of the North American Brown Bear or Grizzly:**
586 ***Ursus arctos* ssp. *horribilis*.** *Genes (Basel)* 2018, **9**.
- 587 40. Ware JV, Nelson OL, Robbins CT, Jansen HT: **Temporal organization of activity in**
588 **the brown bear (*Ursus arctos*): roles of circadian rhythms, light, and food**
589 **entrainment.** *Am J Physiol Regul Integr Comp Physiol* 2012, **303**:R890-902.
- 590 41. Perteua G, Perteua M: **GFF Utilities: GffRead and GffCompare [version 2; peer review:**
591 **3 approved].** *F1000Research* 2020, **9**.
- 592 42. Kim D, Paggi JM, Park C, Bennett C, Salzberg SL: **Graph-based genome alignment**
593 **and genotyping with HISAT2 and HISAT-genotype.** *Nature Biotechnology* 2019,
594 **37**:907-915.
- 595 43. Bray NL, Pimentel H, Melsted P, Pachter L: **Near-optimal probabilistic RNA-seq**
596 **quantification.** *Nat Biotechnol* 2016, **34**:525-527.
- 597 44. de la Fuente L, Arzalluz-Luque A, Tardaguila M, Del Risco H, Marti C, Tarazona S,
598 Salguero P, Scott R, Lerma A, Alastrue-Agudo A, et al: **tappAS: a comprehensive**
599 **computational framework for the analysis of the functional impact of differential**
600 **splicing.** *Genome Biol* 2020, **21**:119.

- 601 45. Mi H, Ebert D, Muruganujan A, Mills C, Albou L-P, Mushayamaha T, Thomas PD:
602 **PANTHER version 16: a revised family classification, tree-based classification tool,**
603 **enhancer regions and extensive API.** *Nucleic Acids Research* 2020, **49**:D394-D403.
604